SF2A 2007
J. Bouvier, A. Chalabaev, C. Charbonnel (eds)

THE POLYCHROMATIC LASER GUIDE STAR : THE ELP-OA DEMONSTRATOR AT OBSERVATOIRE DE HAUTE PROVENCE

R. Foy[1 2], M. Chatagnat[1], D. Dubet[1], P. Éric[2], J. Eysseric[2], F.-C. Foy[1], T. Fusco[3], J. Girard[4], A. Laloge[2], A. Le Van Suu[2], B. Messaoudi[1], S. Perruchot[2], P. Richaud[2], Y. Richaud[2], X. Rondeau[1], M. Tallon[1], É. Thiébaut[1] and M. Boër[2]

Résumé. The correction of the tilt for adaptive optics devices from the only laser guide star can be done with the polychromatic laser guide star. We report the progress of the first demonstrator of the implementation of this concept, at Observatoire de Haute-Provence. We review the last steps of the feasibility studies, the optimization of the laser parameters, and the studies of the implementation at the OHP 1.52m telescope, including the beam propagation to the lasers room to the mesosphere and the algorithms for tip-tilt measurements.

1 Introduction

Adaptive optics (AO) at large telescopes requires a source of reference for phase corrugation measurements. When the source of interest or a close enough natural guide star (NGS) is too faint to provide the AO wavefront sensor with enough light, the phase reference can be a laser guide star (LGS)(Foy & Labeyrie 1985). Unfortunately, the tilt θ of the wavefront is undetermined, simply because one does not know the precise location of the laser spot in the mesosphere (Pilkington 1987 ; Séchaud et al. 1988). To overcome this difficulty, we are developing our concept of polychromatic LGS (PLGS) (Foy et al. 1992 ; Foy et al. 1995 ; Schöck et al. 2002). After having carried out an in-depth feasibility study, we are building a demonstrator of this concept at the 1.52m telescope (Observatoire de Haute-Provence, OHP) : it is the "Étoile Laser Polychromatique pour l'Optique Adaptative" programme (ELP-OA).

The goal of the ELP-OA is to provide us with the tilt measurement, and thus the tilt correction, toward any direction in the sky, without any NGS, i.e. : with a 100% sky coverage, even down to visible wavelengths, where the small isoplanatic brings a dramatic limitation to the use of AO at the telescope diffraction limit. In this paper we will focus on the recent results which we got within the framework of ELP-OA.

2 How will ELP-OA work ?

Let briefly recall the basic concept of the PLGS. It relies on the chromatism of the air refraction index n :

$$n(\lambda, P, T) - 1 = f(\lambda) \times g(P, T) \tag{2.1}$$

where P and T stand for the atmospheric pressure and temperature. It yields :

$$\Delta\, n/(n-1) = \Delta\, f(\lambda)/f(\lambda) \tag{2.2}$$

[1] Université de Lyon, F-69000 Lyon, France ; Centre de Recherche Astrophysique de Lyon, Observatoire de Lyon, 9 avenue Charles André, F-69561 Saint-Genis Laval cedex, France ; CNRS, UMR 5574 ; Ecole Normale Supérieure de Lyon, F-69007 Lyon, France ; Université de Lyon 1, F-69622 Villeurbanne, France ;

[2] Observatoire de Haute-Provence, F-04870 Saint-Michel l'Observatoire ; CNRS, USR 2207

[3] ONERA, BP. 52, 29 avenue de la Division Leclerc, F-92320 Chatillon Cedex

[4] Instituto de Astronomía, Universidad Nacional Autonoma de México, Apdo. Postal 70-264, 04510 México, D. F., México

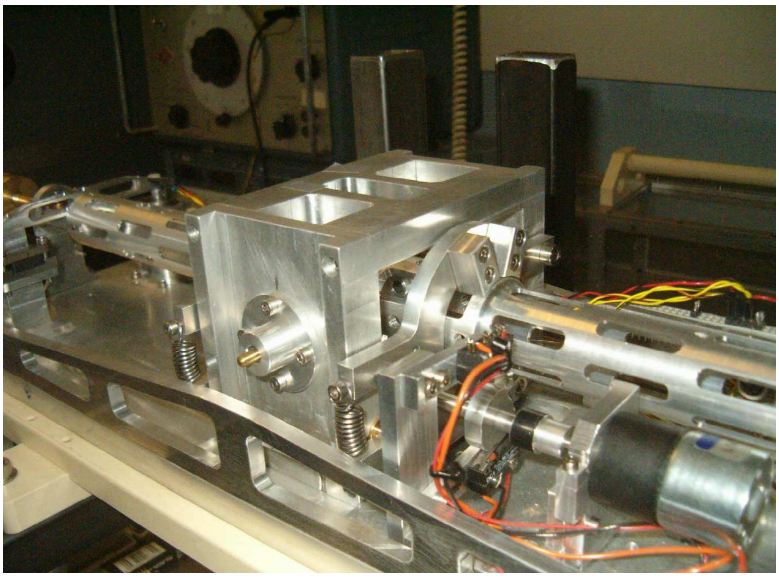

Fig. 1. A pendular seismometer (Tokovinin 2000). The arm is ≈55 cm long

When we applies Eq.2.2 to the tilt θ of the wavefront expansion (the piston term being removed), we get :

$$\theta_{\lambda_3} = \Delta\theta_{\lambda_1,\lambda_2}(n_{\lambda_3} - 1)/\Delta n_{\lambda_1,\lambda_2}. \tag{2.3}$$

Thus the tilt at any wavelength λ_3 can be derived from the tilt difference between two wavelengths λ_1 and λ_2. The larger the wavelength difference and the shorter the shortest wavelength, the higher the differential tilt. The backscattering process relies on the two-photon excitation of the $4D_{5/2}$ energy level of sodium atoms in the mesosphere. It produces a line spectrum ranging from 330 nm, close to the ozone atmospheric transmission cut-off, up to 2.34 μm. Two laser chains will raise the valence electrons first from the ground level to the $3P_{3/2}$ energy level through the 589 nm (D_2 transition) and second from that level to the $4D_{5/2}$ one through the 569 nm transition.

Very likely we will use lasers from the French CEA isotopic separation programme SILVA/MENPHIS, which is now completed. They are made up of phase modulated dye lasers pumped by NdYAGs. The nominal average power $< P >$ per wavelength will be 34 W at the chain output, and 22 W at the mesosphere. If required, we will be able to increase twofold $< P >$ for both spectral channels.

To get the maximum sensitivity, we will measure the differential tilt $\Delta\theta$ between 0.330 nm and 2.34 μm.

The PLGS relies on the measurement of differential parameters, up to now the centers of gravity. Therefore the tilt derived from $\Delta\theta$ is not sensitive to telescope vibrations, jumps, drifts, ..., whereas the tilt is. Thus we have to measure these telescope movements synchronously with the the differential tilt. It will be done with pendular seismometers (Tokovinin 2000), which measure angles with a standard deviation of ≈3 marcsec (Fig. 1). Two of them have been built, one per telescope axis. An upgraded version is almost completed, with improved robustness and a wider bandwidth, in particular toward low frequencies.

3 Laser - sodium interaction

CEA has developed the code BEACON for the two-photon excitation of sodium. It computes the return flux from the mesosphere. BEACON is based on density matrix formalism to solve the optical Bloch equations (Bellanger et al. 2004). Curves of growth of the return flux at 330 nm computed with BEACON are shown in Fig. 2, assuming that both two laser beams at 589 and 569 nm have equal density powers, are circularly polarized, have gaussian pulse profiles, and are phase modulated to span 3 and 1 GHz respectively. Parameters of the two sine functions of each phase modulator have been optimized to closely match the Doppler + hyperfine structure and Doppler profiles respectively. Note that even at saturation, one has to take into account the pulse width when deriving the return flux from the density power. This is because the return flux depends on the number of excitation cycles up to the $3P_{3/2}$ level during the pulse.

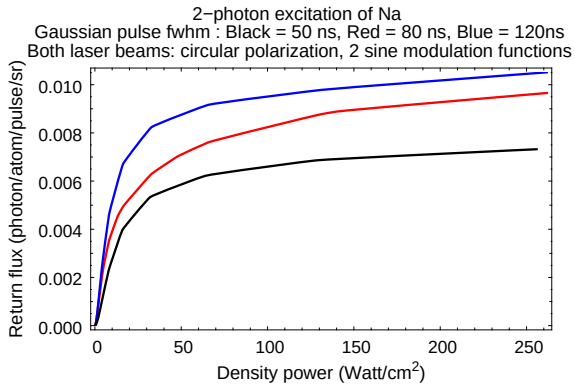

Fig. 2. Curve of growth of the return flux at 330 nm from the resonant two-photon excitation of the $4D_{5/2}$ energy level of sodium, for different pulse durations. Computed with the BEACON code of CEA (Bellanger et al. 2004).

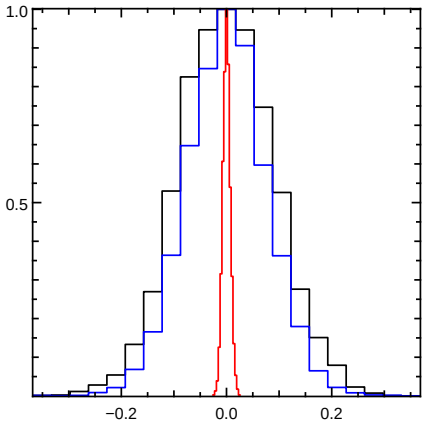

Fig. 3. Distribution of the error in θ measurements. From outer to inner curves : center of gravity, cross spectrum, cross spectrum with phase restoration. x axis : pixel unit. It assumes the LGS spot is not resolved.

We have simulated the spatial energy distribution in the mesosphere. Coupling it with curves of growth as those in Fig 2, we have mapped the backscattered photons both at 330 nm and at 2.3 μm. To get the 2.2 + 2.34 μm map, we have simply scaled the 330 nm map with the branching ratio of the radiative decay between these two wavelengths. We have assumed that the detector for the 330 nm channel is an EMCCD with a typical readout noise of 0.3 e^-/pixel, and that the readout noise of the IR channel is 10 e^-/pixel. These parameters are not critical, since we are close to purely photon noise regime.

Global efficiency is ≈0.09 at 330 nm, and 0.20 at 2.3 μm, including the atmosphere, the telescope (with dedicated coatings for the M2, M3 and M4 mirrors), optics and detectors.

4 Methods of differential tilt measurement

The simplest way to measure the differential tilt is to measure the difference in the center of gravities of the chromatic components of the PLGS image at the focus of the master (1.52 m) telescope. The accuracy in the measurement $\sigma(\theta)$ is limited by the seeing disk fwhm $\approx \lambda/r_0$, where r_0 stands for the Fried parameter and the number of photons in the image N_{ph} :

$$\sigma(\theta) \approx \lambda/(r_0 \times \sqrt{N_{ph}}) \tag{4.1}$$

The differential tilt measured in this way is not accurate enough to allow us to derive θ at $\pm\lambda/D$ (Schöck et al. 2002) ; it is mandatory that the master telescope is equipped with an AO device if the tilt is computed in this way, or that we use a better algorithm. Also, the diameter d of the launch telescope should be such that the profile of the laser energy distribution in the mesosphere is dominated by a bright speckle, unless it is equipped with an AO, which is quite unrealistic for ELP-OA. Thus, $d \lesssim 3 \times \lambda_{laser}/r_0(\lambda_{laser})$.

Much better performances can be obtained if one uses an algorithm which reaches the limit imposed by the Cramèr Rao criterion. In this case, $\sigma(\theta)$ is limited by the size of the convolution of the spot size with the Airy disk of the master telescope. A first step toward this goal is to compute the cross spectrum of images at two different wavelengths λ_i. Since the speckle patterns are different, the gain achievable with this method comes from the lower orders of the wavefront. The distribution of the error in θ measurements is shown in Fig. 3, compared to the center of gravity case.

Phase restoration from the speckled images is able to reach the Cramèr Rao criterion. Indeed, for a given point of the wavefront, the optical paths are almost equal whatever the wavelength, and the phases differ by a linear factor of λ. One cannot crosscorrelate the speckle patterns, but we can crosscorrelate the wavefronts. It has been demonstrated to be very efficient, up to $D/r_0 \approx 70$ (Rondeau, 2007 ; Rondeau et al. 2007). The inner curve of Fig. 3 shows the tilt error distribution with such an algorithm, on the case of a point source again. Today, it is not fast enough for real time applications.

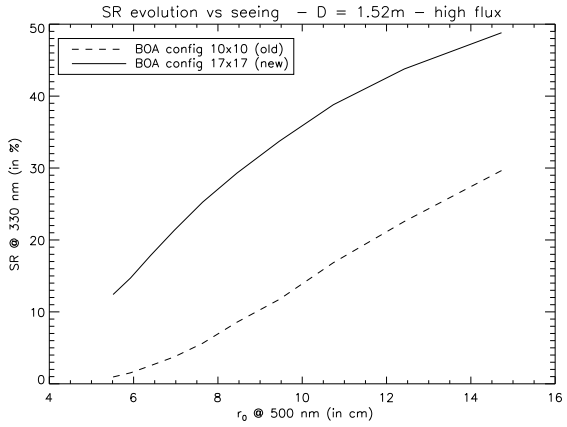

Fig. 4. Strehl ratio at 330 nm predicted for the BOA adaptive optics bench of ONERA at the coudé focus of the 1.52 m telescope at Observatoire de Haute-Provence.

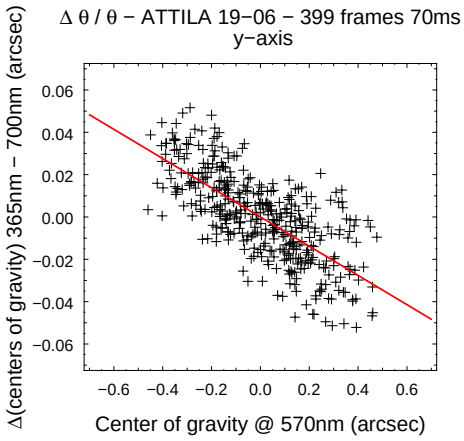

Fig. 5. Differential tilt versus tilt. Orthogonal regression line.

5 The launch telescope

The gain of the polychromatic phase restoration method is limited by the size of the laser spot in the mesosphere, or by the size of its smallest features, i.e. by the speckle pattern of the laser beams at the mesosphere. Consequently the launch projector will be a ≈40 cm refractor. Indeed crosscorrelation of the speckles of the chromatic components of the laser spot will be beneficial as long as they are resolved by the master telescope, from where we have

$$d \leqslant D \times \lambda_{min}/\lambda_{max} \longrightarrow d \leqslant 0.4\text{m} \tag{5.1}$$

with D = 1.52 m, λ_{min}=0.33 nm and λ_{max}= 2.34 μm. We are studying the case of larger projectors with super-resolution for the 2.3 μm component image ; there is a trade-off between the gain resulting from the larger d and a loss due to the lower contrast of speckle pattern at 2.3 μm.

6 Adaptive Optics

The BOA adaptive optics bench, from ONERA (France) will be installed at the coudé focus of the master telescope. It is currently being upgraded from 10^2 to 17^2 actuators. Figure 4 shows the comparison of the old and new configurations in the case of high flux. The wavefront sensor will be fed by the return flux within the $D_1 + D_2$ NaI lines (expected equivalent V magnitude : ≈7.8 for $< P >=$ 22 W). We have assumed that BOA provides in fact $\mathcal{S} = 1$; this assumption is almost valid at 2.3 μm. At 330 nm, $\mathcal{S}_{330nm} \approx 0.3$ from Fig. 4 ; we are currently simulating the effect of $\mathcal{S}_{330nm} < 1$.

7 ATTILA : on the sky check of the θ measurement accuracy

The ATTILA experiment aimed at checking the feasibility of the measurement of θ at the required accuracy. Indeed diffraction limited imaging requires $\sigma_\theta \lesssim 1 \times \lambda/D$, where D stands for the master telescope diameter. ATTILA has used NGSs to simulate a PLGS. An optics setup has been installed at the coudé focus of the OHP 1.52 m telescope. The coudé beam was collimated and then split into 4 wavelength channels, and finally 4 narrow bandwidth images were formed onto an EMCCD Roper camera (Foy et al. 2003 ; Girard, 2005). Multiplication gains of 30 to 100 allowed us to drop the readout noise to 0.5 - 1 e^-/pixel, which is negligible with respect to photon and multiplication noises. Exposure times were 70 ms. Differential tilts were measured from an improved iterative center of gravity algorithm applied to the seeing disk.

Figure 5 shows the correlation between the differential tilt $\theta_{365} - \theta_{700}$ and the tilt θ_{570} at 570 nm. The slope of the relation is ≈2 times higher than expected from the variation of n. This is due to magnifying factors slightly different for the wavelength channels, and which are not corrected here. Note that θ_{570} measurements include the contribution of telescope movements (vibrations, jumps, wind shakes, ...), whereas $\theta_{365} - \theta_{700}$ ones

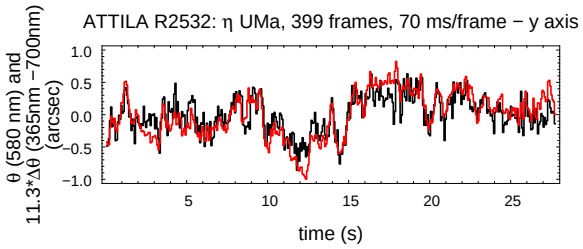

Fig. 6. Tilt derived from the differential tilt between 365 and 700 nm versus time (black line). Red or gray : tilt measured at 580 nm.

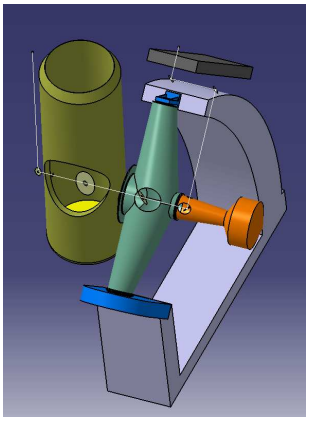

Fig. 7. Optical path of the laser beam to reach the launch projector mated to the OHP 1.52 m telescope

do not. The tilt derived from the differential tilt correlates nicely with the tilt (Fig. 6). Again, on this figure also, the tilt plot is affected by telescope movements, whereas the tilt derived from $\delta\theta$ is not, which contributes to the small differences between the two plots.

We have checked from the data that we are shot noise limited (photon noise *and* multiplication noise). Typically, we have measured $\sigma_\theta \approx 1.5\lambda_{550}/D$, so slightly more than the Airy disk fwhm in the V photometric band. The number of photons detected per frame was typically 4×10^5 in the uv. The seeing was ≈2", i.e. $r_0(365nm) \approx 3.4$ cm and the uv seeing ≈2.2". The center of gravity is applied instead to the width of the disk seeing λ/r_0. If it was applied to speckle features (which is equivalent to a crosscorrelation or to a phase restoration) convolved with the laser speckle pattern produced at the mesosphere by a $d = 0.4$ m launch telescope, the width would have been $\lambda/(0.4 \times 4.85 \times 10^{-6}) \approx 0.19''$. It means that we would approximately get the same σ_θ with $(d/r_0)^2 \approx 140$ times less photons, i.e. : ≈2900 photons. It is close to the ≈3000 detected return flux predicted for ELP-OA (see section 3). Thus ATTILA results confirm the feasibility of ELP-OA.

8 The ELP-OA demonstrator at OHP

The laser chains will rely on dye technology, since today there is no other way to produce the required power at 569 nm. This is the technology developed of isotopic separation programmes, in particular at LLNL in the USA and by CEA in France. The three stages, oscillator, preamplifier and amplifier, will be pumped with diode-pumped Nd-YAG lasers. The dye circulators will be those developed by CEA or a copy of them. We have chosen to run the two chains in co-amplification, so that the amplifier is common to both chains.

Specifications are :

- Output average power per chain : 34 W (leading to ≈22 W at the mesosphere), possibly up to 68 W
- Pulse length : $\gtrsim$ 80 ns
- Repetition rate : 20 kHz
- Output beam diameter : ≈1 mm
- Output beam aspect ratio : 5×7, tbc
- Beam quality : such as the beam spot energy distribution at the mesosphere is seeing limited
- Optical throughput of the preamplifiers : 17%
- Optical throughput of the amplifier : 45%

The amplifier will be installed in an insulated room in the dome, close to the North pillar of the telescope.

The launch telescope will be mated along the telescope tube. The telescope mount is an English type one. The beam to be injected into the launch projector will enter the telescope mount through the hour angle axis, on its North side (the South side is used to feed the coudé focus, as usual for this type of mount). Then, (see Fig. 7) after a detour for technical reasons, the beam will enter the declination axis. It will cross the center of the M4 mirror (inside the central obscuration), will cross the telescope tube and then will reach the projector. This optical path design allows us to propagate the laser beam without any fiber optics (which are not yet really available without significant losses) or moving mirrors (which raise problems for baffling and for keeping

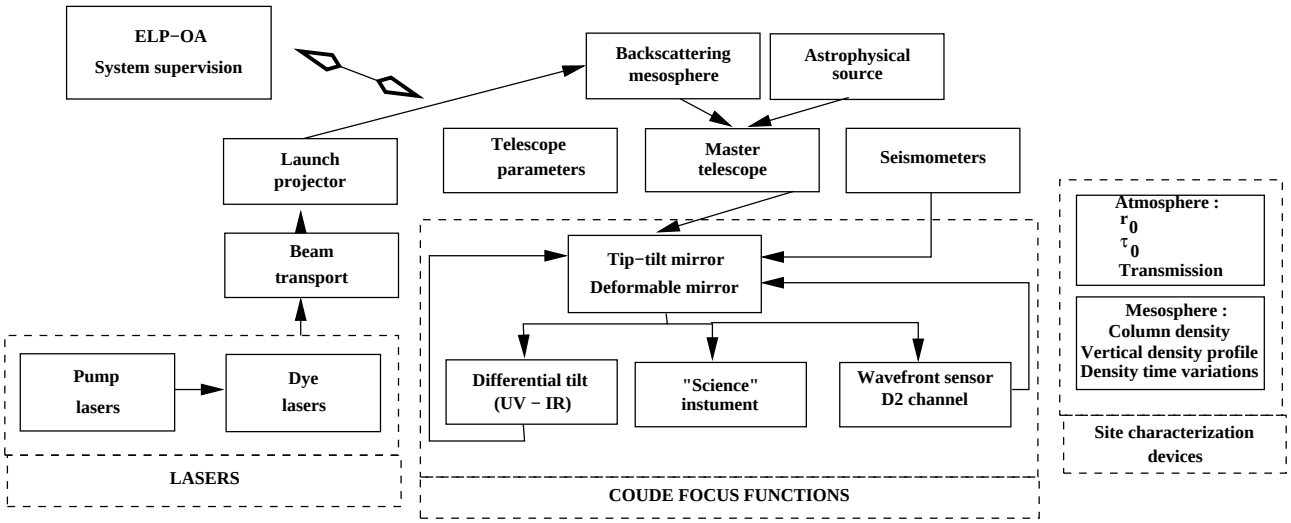

Fig. 8. Global functional diagram of the ELP-OA demonstrator.

constant the polarization). This design could be implemented on any type of mount, at least if ever it has been taken into account in the telescope design.

The global scheme of the demonstrator is summarized in Fig. 8. In addition to the above devices, the coudé focus setup will host a science instrument which will be use to characterize the performances of the whole system, in particularly through long exposure at the highest spatial resolution.

External devices will measure the required parameters to fully model the performances. The atmosphere transparency, r_0 and the seeing correlation time τ_0 will be measured with a Generalized Seeing Monitor (GSM) (Conan et al. 1999) simultaneously with the ELP-OA observations. From another telescope at OHP, mesospheric relevant parameters will be measured : sodium column density, vertical sodium density and their time variations.

Implementations studies at the 1.52 m telescope and building are running. All matters related to the use of high power laser directed to the sky are being addressed : security of the personnel on the site, aircraft traffic, satellites. Upgrade of the power supply equipment to be able to feed the pump lasers and the cooling have been done. We plan to have the first launch of the 589 nm beam at zenith by the end of 2008, and to start the full operation from the end of 2009.

We thank the staff of Observatoire de Haute-Provence, and CNRS/INSU for their support. This project is funded by ANR (contract NT05-4_41579), CNRS/INSU/CSA, DGA (contract 06-34046) and PACA Region (contract 2006_20307).

Références

Bellanger V., Courcelle A., Petit A., 2004, Computer Physics Communications, 162, 143

Conan R., Ziad A., Tokovinin A., et al., 1999, Measurement of the optical relevant parameters for high angular resolution astronomy with the Generalized Seeing Monitor(G.S.M.), in A.S.P. Conf Ser, 174, 27

Foy R., Boucher Y., Fleury B., et al., 1992, ATLAS status report and tilt sensing using multicolour laser reference star, ESO Conf. 42, 437

Foy R., Girard J., Tallon M., et al., 2003, Polychromatic Laser Guide Star. Progress report, in Combes F., Barret D., Contini T., Pagani L. (eds.), SF2A Semaine de l'Astrophysique Francaise

Foy R., Labeyrie A., 1985, AA, 152, L29

Foy R., Migus A., Biraben F., et al., 1995, Astron. Astrophys. Suppl. Ser., 111, 569

Girard J., 2005, Ph.D. thesis, Université Claude Bernard Lyon 1, Villeurbanne, France

Pilkington J., 1987, Nature, 330, 116

Rondeau X., Thiébaut E., Tallon M., Foy R., 2007, Journal of the Optical Society of America A, 24

Rondeau X., 2007, Ph.D. thesis, Université Claude Bernard Lyon 1, Villeurbanne, France

Schöck M., Foy R., Tallon M., Noethe L., Pique J.-P., 2002, MNRAS, 337, 910

Tokovinin A., 2000, MNRAS, 316, 637